Paracellular transport of phosphate along the intestine

Knöpfel, Thomas ; Himmerkus, Nina ; Günzel, Dorothee ; Bleich, Markus ; Hernando, Nati ; Wagner, Carsten A

Abstract: Inorganic phosphate (P) is crucial for many biological functions, such as energy metabolism, signal transduction, and pH buffering. Efficient systems must exist to ensure sufficient supply for the body of P from diet. Previous experiments in humans and rodents suggest that two pathways for the absorption of P exist, an active transcellular P transport and a second paracellular pathway. Whereas the identity, role, and regulation of active P transport have been extensively studied, much less is known about the properties of the paracellular pathway. In Ussing chamber experiments, we characterized paracellular intestinal P permeabilities and fluxes. Dilution potential measurements in intestinal cell culture models demonstrated that the tight junction is permeable to P, with monovalent P having a higher permeability than divalent P. These findings were confirmed in rat and mouse intestinal segments by use of Ussing chambers and a combination of dilution potential measurements and fluxes of radiolabeled P. Both techniques yielded very similar results, showing that paracellular P fluxes were bidirectional and that P permeability was 50% of the permeability for Na or Cl. P fluxes were a function of the concentration gradient and P species (mono- vs. divalent P). In mice lacking the active transcellular P transport component sodium-dependent P transporter NaPi-IIb, the paracellular pathway was not upregulated. In summary, the small and large intestines have a very high paracellular P permeability, which may favor monovalent P fluxes and allow efficient uptake of P even in the absence of active transcellular P uptake. The paracellular permeability for phosphate is high along the entire axis of the small and large intestine. There is a slight preference for monovalent phosphate. Paracellular phosphate fluxes do not increase when transcellular phosphate transport is genetically abolished. Paracellular phosphate transport may be an important target for therapies aiming to reduce intestinal phosphate absorption.

DOI: https://doi.org/10.1152/ajpgi.00032.2019

Paracellular transport of phosphate along the intestine

Thomas Knöpfel[1], Nina Himmerkus[2], Dorothee Günzel[3], Markus Bleich[2], Nati Hernando[1], Carsten A. Wagner[1]

[1]University of Zürich, Institute of Physiology - Zürich, Switzerland
[2]Christian-Albrechts-Universität zu Kiel, Physiologisches Institut - Kiel, Germany
[3]Charité - Universitätsmedizin Berlin, Campus Benjamin Franklin, Institut für Klinische Physiologie - Berlin, Germany

Key words: Intestinal absorption, phosphate, paracellular transport, NaPi-IIb

Corresponding author:
Carsten A. Wagner
Institute of Physiology
University of Zurich
Winterthurerstrasse 190
CH-8057 Zurich
Switzerland
Email: Wagnerca@access.uzh.ch
Phone: +41-44-63 55023
Fax: +41-44-63 56814

Abstract

Inorganic phosphate (P_i) is crucial for many biological functions such as energy metabolism, signal transduction and pH buffering. Efficient systems must exist to ensure sufficient supply of the body with P_i from diet. Previous experiments in humans and rodents suggest that two pathways for the absorption of P_i exist, an active transcellular P_i transport and a second paracellular pathway. Whereas the identity, role and regulation of active P_i transport has been extensively studied, much less is known about the properties of the paracellular pathway.

In Ussing chamber experiments we characterized paracellular intestinal P_i permeabilities and fluxes. Dilution potential measurements in intestinal cell culture models demonstrated that the tight junction was permeable to P_i, with monovalent P_i having a higher permeability than divalent P_i. These findings were confirmed in rat and mouse intestinal segments using Ussing chambers and a combination of dilution potential measurements and fluxes of radiolabeled $^{32}P_i$. Both techniques yielded very similar results showing that paracellular P_i fluxes were bidirectional and that P_i permeability was about 50% of the permeability for Na^+ or Cl^-. P_i fluxes were a function of the concentration gradientand P_i species (mono- vs. divalent P_i). In mice lacking the active transcellular P_i transport component, NaPi-IIb, the paracellular pathway was not upregulated.

In summary, the small and large intestine have a very high paracellular P_i permeability that may favour monovalent P_i fluxes and allows efficient uptake of P_i even in the absence of active transcellular P_i uptake.

Introduction

Maintaining homeostasis of inorganic phosphate (P_i) is crucial for many physiological, structural and cellular functions and is achieved by coordinated absorption of P_i in the small intestine and reabsorption in the kidney, whereas bone functions mostly as a storage compartment. This system is tightly regulated by a hormonal network, where active vitamin D_3 stimulates intestinal P_i absorption (4, 15, 17) while fibroblast growth factor 23 (FGF23) and parathyroid hormone (PTH) inhibit renal reabsorption facilitating the excretion of excessive P_i (2, 21). Disturbance of P_i balance results in a variety of pathological states and can occur either as a consequence of rare monogenic disorders, poor nutrition, intestinal disease, as side effects of drugs in patients with transplanted organs, or in patients suffering from chronic kidney disease (CKD) (20). Hypophosphatemia, often caused by genetic disorders leading to renal P_i wasting (for review see (1, 42)), frequently results in abnormal skeletal formation and rickets. On the other hand hyperphosphatemia is associated with increased cardiovascular morbidity and mortality in the general population but even more so in patients with CKD (35). In fact, disturbed P_i homeostasis occurs early on in the progression of CKD due to the diminished glomerular filtration and the consequent inability of the kidney to excrete P_i (20).

The impact of dietary P_i content has been granted little attention until recently, when P_i was associated with premature aging, vascular calcifications, cardiovascular mortality, risk for renal failure, and bone damage in the general population (31, 37). Therefore it is of importance to better understand the mechanisms underlying intestinal P_i absorption. Though hyperphosphatemia is considered to be a risk factor, still our daily intake of P_i exceeds recommended amounts (3). The increased dietary intake of P_i is partially attributed to the consumption of processed food and soft drinks, since preservatives in these products contain a high amount of P_i salts. In contrast to phosphate species (i.e. organic phytophosphates) naturally present in the food, these additives have a much higher availability for absorption (24). This high amount of P_i in our nutrition is expected to provide a strong diffusion gradient across the intestinal epithelium.

Dietary P_i is mainly absorbed in the small intestine. Early reports indicated that an intragastric bolus of P_i in rats increased plasma P_i levels linearly with increasing P_i concentration of the bolus (33). Further experiments in Ussing chambers with rat

jejunum suggested a two component transport, with a linear relationship between transport and substrate at luminal P_i concentrations above 1 mM, whereas below 1 mM P_i transport appeared more complex. At low concentrations an active intestinal P_i transport system therefore seemed more likely since a passive system alone would cause P_i efflux from blood into the intestinal lumen following its chemical gradient (43). These observations, also confirmed in intestinal transport studies in humans (34, 44), led to a model that intestinal transport of P_i proceeds via two distinct mechanisms: one component is active and sodium dependent and appears to saturate at low P_i concentrations (43), whereas the second mechanism solely relies on the luminal P_i concentration and does not show saturation resembling passive diffusion (33). The latter system may have a higher capacity than the active transport system.

Active transcellular transport of P_i is mostly mediated by the sodium dependent P_i transporter NaPi-IIb (SLC34A2) (17, 18), which is expressed at the luminal side of enterocytes in the small intestine (36). The abundance of NaPi-IIb is regulated by dietary P_i content (15, 29) and vitamin D_3 (4, 25), with dietary P_i restriction and vitamin D_3 increasing the cotransporter expression levels. The total knock out of NaPi-IIb is lethal (41), however, in a tamoxifen inducible model (39) as well as in our own intestine-specific NaPi-IIb knock out (KO) (16, 27) the contribution of this transporter could be investigated. Indeed NaPi-IIb appears to be the major P_i transporter in the intestine since P_i transport into everted intestinal sacks and brush border membrane vesicles (BBMV) was nearly abolished in the absence of NaPi-IIb, causing higher fecal P_i excretion (16, 39). Due to increased renal P_i reabsorption these mice are able to maintain normal plasma P_i levels when fed standard chow, resulting in a in a rather mild phenotype despite the lack of active intestinal transport (16, 39). Moreover, patients with mutations in the SLC34A2 gene suffer from pulmonary alveolar microlithiasis (PAM), but no alterations of plasma P_i or hormonal levels have been reported (5). However, NaPi-IIb KO mice become transiently hypophosphatemic and resorb bone to compensate for the insufficient intestinal supply when challenged with a low P_i diet suggesting an important role of NaPi-IIb under conditions of P_i-deprivation (27).

In addition to the mild phenotype in the absence of intestinal NaPi-IIb, several observations further support the presence of alternative pathways for intestinal

116 absorption of P_i. First, administration of a high P_i diet to both, wild type (WT) and
117 NaPi-IIb KO mice results in a drastic increase in urinary excretion of P_i, reflecting a
118 higher delivery of P_i from the intestine, despite the fact that expression of NaPi-IIb is
119 decreased under high dietary P_i load (WT) or absent (KO) (36). Second, in adenine
120 treated animals, a model for CKD, the absence of NaPi-IIb alone is not able to
121 prevent hyperphosphatemia; instead, normalization of plasma P_i levels requires the
122 treatment with sevelamer, a P_i binder (40). Altogether, these data suggests that
123 NaPi-IIb is essential to scavenge P_i when the luminal concentration of P_i is low, a role
124 supported by the low K_m of the cotransporter for P_i (about 10 µM) (9), whereas under
125 normal and high dietary P_i supply the electrochemical gradient of P_i across the
126 intestinal epithelium would favor passive absorption through the paracellular pathway
127 as even at P_i (lumen) < Pi (blood) the lumen negative potential could drive P_i
128 absorption. Indeed, under normal dietary conditions luminal P_i concentrations exceed
129 the levels in serum several fold (32), thus creating a gradient driving passive
130 absorption of P_i, which might explain the mild phenotype of NaPi-IIb KO mice and the
131 normal plasma P_i levels in PAM patients (27). The functional characteristics and
132 molecular mechanism(s) responsible for passive P_i absorption are largely unknown.

133 Selective paracellular permeability is controlled by several components of tight
134 junctions, among which the claudin family has been shown to be involved in gating
135 passive diffusion for several ions across epithelia (for review see (14)). So far, no
136 association of a particular claudin to paracellular Pi transport has been identified.
137 Since conductance of tight junctions is selective for size and charge (11, 12), one
138 needs to consider that two P_i ionic species are present under physiological conditions
139 (monovalent $H_2PO_4^-$ and divalent HPO_4^{2-}), and that tight junctions (similar to NaPi-IIb)
140 might favor one particular ion

141 In this study we analyzed the paracellular P_i transport properties of several intestinal
142 cell culture models as well as of the different intestinal segments of rats and mice,
143 and show that the tight junctions are indeed permeable to P_i and mildly discriminate
144 between monovalent and divalent P_i species.

145

Methods

Ethical approval

All animal experiments were approved by the local veterinary authority (Veterinäramt Zürich) and performed according to Swiss Animal Welfare laws. The authors confirm that this study is in agreement with the guidelines of the *The Journal of Physiology* (13).

Animal and Tissue handling

Experiments were done in two month old Wistar rats (Janvier, France) as well as in floxed-Slc34a2 male mice expressing villin-driven Cre recombinase (KO, NaPi-IIb$^{f/f}$) (16) and their wild type litter mates (WT, NaPi-IIb$^{Wt/Wt}$) bred in-house. Animals were fed normal diets (0.8 % Pi, 1 % calcium) (Kliba Promivi AG, Switzerland) ad libitum with free access to water and were kept at a 12 h light and dark cycle. Mice and rats were anesthetized with vaporized isoflurane (3-4%, with an oxygen flow rate of 0.8 l/min) for terminal organ extraction; intestinal tissue was harvested and transferred to oxygenized Ringer solution (145 mM NaCl, 0.4 mM KH_2PO_4, 1.6 mM K_2HPO_4, 5 mM glucose, 1 mM $MgCl_2$, 1.3 mM Ca-Gluconate, pH7.4). Isolated intestinal segments were flushed with Ringer solution, opened longitudinally and mounted on tissue holders for insertion into the Ussing chambers.

Pi determination of intestinal content

Luminal content from different intestinal segments of WT mice fed a standard diet was dissolved in 0.6 M HCl (100 mg/ml), homogenized and centrifuged as reported previously for fecal Pi determination (39). Pi concentration of intestinal content was colorimetrically determined according to the Fiske Subbarow method (8).

Dilution potential measurement in cell culture models, rat and mouse intestine

Dilution potential measurements were performed in modified Ussing chambers. The permeabilities for Na^+ (P_{Na}), Cl^- (P_{Cl}) and Pi (P_{Pi}) of intestinal cell culture models and intestinal segments were determined in Ussing chambers with a bubble lift system gassed with oxygen, that drives the circulation of the bathing solutions (10 ml) on each side, in which the basolateral and apical sides were independently perfused and temperature was maintained at 37°C with a water jacket as previously described (38). This analysis was performed in IPEC-J2 (porcine small intestine), HT-29/B6,

Caco2-bbe and T84 cells (the last three of human colon carcinoma origin) grown to confluency on culture plate inserts (Millicell PCF filters, pore size 0.4 µm, effective area 0.6 cm^2) as well as on rat intestinal tissue (effective area 0.28 cm^2) prepared as described above. Experiments were performed in a solution containing (in mM) 140 NaCl, 5.4 KCl, 1 $MgCl_2$, 1.2 $CaCl_2$ and 10 glucose, with pH adjusted either to pH 6 (10 mM MES/NaOH) or pH 8.4 (10 mM TAPS/NaOH). To determine the permeabilities for Na^+ and Cl^-, 5 ml from either the basolateral or apical side was replaced by 5 ml of a solution containing 280 mM mannitol instead of 140 mM NaCl. After equilibrating each side again, the permeability for P_i was then assessed by replacing 5 ml on either side with a solution containing 140 mM NaH_2PO_4 (pH 6) or 70 mM Na_2HPO_4 (pH 8.4, with additional 70 mM mannitol to maintain osmolality) instead of 140 mM NaCl.

For dilution potential measurements in mouse intestine a modified Ussing chamber with a flow through system was used, where basolateral and apical side were independently and continuously perfused with a flow rate of 5-10 ml/min (19). Perfused and freshly isolated intestinal segments from mouse were mounted into the Ussing chamber, with an exposed area of 0.8 mm^2. The basolateral side was perfused with Ringer solution adjusted at pH 7.4. After equilibration of the mounted tissue, the apical side was consecutively perfused with standard Ringer solution (145 mM NaCl, pH 6), a low NaCl Ringer (30 mM NaCl, supplemented with 230 mM Mannitol, pH 6), and a modified Ringer (140 mM NaH_2PO_4, pH 6).

Differences in V_{te} upon changes of perfusion solution were measured under open-circuit conditions and corrected for previously defined liquid junction potentials, with V_{te} referring to the apical side for rat and cell culture models and to the basolateral side in mouse. R_{te} was assessed with short pulses (1s) of 1.41 µA, and the difference in V_{te} upon the pulse was used to calculate the R_{te} according to Ohm's law ($R_{te}=\Delta V_{te}/I$) after correction for the resistance of the empty chamber. Relative and absolute permeabilities for Na^+, Cl^- and Pi were calculated using the Goldman-Hodgkin-Katz equation and R_{te}. The ratios P_{Na}/P_{Cl} and P_{Na}/P_{Pi} were obtained by the Goldman-Hodgkin-Katz equation and the transepithelial resistance (R_{te}) was used to calculate absolute permeabilities (26).

Flux measurements

Pi fluxes in rat jejunum and different intestinal segments of WT and NaPi-IIb KO mice were measured in an Ussing chamber with bubble lift system. Two different protocols were applied to distinguish between accumulation and equilibration of P_i. The first one was similar to the protocol described above for dilution potential measurements (zero-trans experiments). Solutions were buffered with Pi and a gradient of 10, 35 and 70 mM (only pH 6) in presence of ^{32}P-phosphate was applied from apical to basolateral bath or *vice versa*. In the second protocol an equilibrium exchange experiment was performed in which tissue was equilibrated in modified Ringer with equal amounts of Pi (10, 35 and 70 mM) on both sides and ^{32}P-phosphate present only on one side for half an hour. In both protocols samples from the acceptor side were taken as blank values before addition of the radioactive tracer to the donor side. Samples were then collected at different time points (10, 20, 30, 60, 90, 120, 180 and 240 minutes); to avoid changes in hydrostatic pressure, equal volumes were removed from the apical and basolateral bath. ^{32}P-phosphate transported to the acceptor side of the tissue was quantified using a β-counter (Packard BioScience).

Statistical Analysis

Unpaired student's t-test or two-way ANOVA with Bonferroni correction for grouped analysis were used to analyze comparisons. P-values < 0.05 were considered as significant. Data is presented as Mean ± SD.

231 ## Results

232 ### Intestinal cell culture models exhibit a paracellular Pi permeability

233 Passive absorption of Pi along the paracellular pathway requires a concentration
234 gradient across the epithelium. Therefore the luminal concentration of P_i in the
235 different segments of the gut of WT mice was determined. As shown in Figure 1A,
236 intraluminal P_i values of mice on a standard diet containing 0.8 % P_i ranged from 14-
237 40 mM, thus largely exceeding plasma levels (2 to 3 mM) (16, 27) (Figure 1A), thus
238 providing a sufficient gradient to drive passive diffusion of P_i from the lumen to the
239 blood.

240 IPEC-J2 as well as HT-29/B6, Caco2-bbe and T84 cells were analyzed in Ussing
241 chambers to determine the permeability of the tight junctions to Na^+, Cl^- and P_i. Tight
242 junction proteins are known to discriminate for size and charge of ions (14); hence
243 experiments were conducted at pH 6 and pH 8.4 to examine if the paracellular
244 pathway was selective for one of the P_i ions present under physiological conditions
245 ($H_2PO_4^-$ and HPO_4^{2-}). At the pH values chosen, more than 95 % of P_i is present either
246 as monovalent P_i (pH 6) or as divalent P_i (pH 8.4). As shown in Figure 1B, alkaline
247 pH of 8.4 tended to lower transepithelial resistance in all models tested, although the
248 reduction reached statistical significance only in T84 cells. Because differences in
249 transepithelial resistance affect the absolute permeability for all ions, permeability
250 results are presented as relative values (P_{Na}/P_{Cl} and P_{Pi}/P_{Na}). The tight junctions of all
251 four intestinal models were permeable for Na^+, Cl^- and P_i (Figures 1C-D). The ratio
252 between the permeabilities of Cl^- and Na^+ seemed to be unaffected by pH (Figure
253 1C) whereas tight junctions discriminated between P_i species (Figure 1D):
254 monovalent P_i ($H_2PO_4^-$), the predominant species at pH 6 passed the tight junctions
255 of all tested cell culture models more efficiently than its divalent form (HPO_4^{2-}). The
256 permeability for P_i at pH 6 was about 40-50% of the one of Na^+.

257 ### Dilution potential measurements in rat intestine demonstrate high
258 ### paracellular P_i permeability

259 The same experimental protocol was used to measure P_i permeabilities in rat
260 jejunum, ileum and distal colon. Comparable transepithelial resistances were
261 measured in jejunum and ileum, whereas a tendency for higher values was observed
262 in colon (Figure 2A). Unlike in cell culture experiments, pH changes did not affect

transepithelial resistance of freshly isolated intestinal tissue (Figure 2A). Dilution potential measurements indicated that the P_{Na}/P_{Cl} ratio was comparable in both small intestinal segments and was unaffected by pH, whereas in the colon the P_{Na}/P_{Cl} ratio was slightly increased at pH 8.4 (Figure 2B). As illustrated in Figure 2C, the rat intestine was also permeable to P_i, with P_{Pi}/P_{Na} ratios higher (about +50 %) at pH 6 than pH 8.4 (though to a lesser extent than observed in the cell culture models); P_{Pi}/P_{Na} ratios were similar in all intestinal segments (Figure 2C). Jejunum and ileum had similar absolute permeabilities for all ions, whereas due to its higher resistance the colon had the smallest values (Figures 2D-F). Absolute P_{Na} (Figure 2D) and P_{Cl} (Figure 2E) were not affected by changes in pH. In contrast, P_{Pi} showed a tendency to be lower at pH 8.4, with the reduction reaching significance only in ileum (Figure 2F).

Paracellular P_i fluxes in rat jejunum exhibit similar characteristics as P_i dilution potentials

In order to validate our observations from dilution potential measurements, radiolabeled flux experiments in Ussing chambers using rat jejunum were performed. In the nominal absence of basolateral P_i, increasing the concentration of P_i at the luminal side (10, 35, and 70 mM, respectively) at pH 6 resulted in increased amounts of $^{32}P_i$ detected at the basolateral side in a time- and concentration-dependent manner (Figure 3A). In absence of a chemical gradient for P_i (similar concentrations of P_i on both sides) transport rates were slightly lower than in the zero-trans experiments, but increased in the same concentration-dependent fashion (Figure 3B). Analyzing average flux rates (average of fluxes from 1 to 4 hour time points), P_i fluxes increased with substrate concentration (Figure 3C). Together, these experiments indicated that the P_i-concentration on the acceptor side changed in a linear fashion with the incubation time and the concentration gradient of the substrate, as expected from passive diffusion. Paracellular transport is considered symmetrical and indeed inverting the gradient (i.e. adding $^{32}P_i$ to the basolateral side (with 10 and 70 mM, respectively) in the nominal absence of luminal P_i) resulted in the same transport rate (Figure 3D), further indicating that the observed flux is driven by simple diffusion. The same experimental procedure was applied to investigate the flux of divalent P_i at pH 8.4 and the concentration of P_i on the acceptor site increased in a time- (Figure 3E) and fluxes increased in a substrate-concentration manner

(Figure 3E) as observed for its monovalent counterpart. Comparison of flux experiments at pH 6 and pH 8.4 revealed increased P_i fluxes at a luminal concentration of 35 mM P_i as well as higher amounts of P_i detected at the basolateral site under acidic conditions for the same substrate concentration (Figure 3G), confirming our earlier permeability findings. Absolute permeability P_{Pi} values for monovalent P_i were higher than for divalent P_i (Figure 3H) and comparable to the observed P_{Pi} in dilution potential measurements (Figure 3I).

The absence of active transcellular phosphate transport does not affect paracellular phosphate permeability

Dilution potential measurements in intestinal segments from WT and NaPi-IIb KO mouse were performed with a luminal pH of 6 and basolateral pH of 7.4 to achieve conditions similar to the *in vivo* situation. The pH difference across the epithelium did not alter the observed transepithelial resistance nor permeabilities (data not shown). Transepithelial resistance tended to be higher in duodenum and colon than in jejunum and ileum, but no differences between WT and KO mice were detected (Figure 4A). P_{Na} (Figure 4A) and P_{Cl} (Figure 4B) followed an inverse trend as resistance, but permeability values of WT and KO animals were comparable. In contrast to rats where P_{Na} and P_{Cl} were about the same, mouse small intestine seems to be more Na^+ selective. P_{Pi} was not altered in NaPi-IIb KO mice, and in both genotypes was highest in ileum (Figure 4D). No differences were observed in relative permeabilities P_{Na}/P_{Cl} (Figure 4E) and P_{Pi}/P_{Na} (Figure 4F).

In order to confirm the data obtained by dilution potential measurements, flux experiments in intestinal segments from NaPi-IIb KO and corresponding WT mice were performed, following the protocol used for flux measurements in rats at pH 6, where overall higher flux rates were observed. As in rats, the amount of $^{32}P_i$ detected at the basolateral side increased with time in a linear fashion in duodenum, jejunum, ileum and colon of mice (data not shown). Moreover, no differences in P_i fluxes were observed between WT and KO mice in duodenum (Figure 5A), jejunum (Figure 5B), ileum (Figure 5C) and colon Figure (5D). The corresponding permeabilities P_{Pi} were calculated from the P_i detected on the basolateral side during these flux experiments. No differences in P_{Pi} were detected between NaPi-IIb deficient and corresponding WT mice during the course of the experiment, reflecting the comparable flux rates observed.. Together, these results suggest that paracellular P_i permeability does not

329 change to compensate for the absence of intestinal NaPi-IIb and concomitant lack of
330 active transport of P_i.

331

Discussion

The mechanisms involved in intestinal P_i absorption are still not fully resolved. Though NaPi-IIb appears to be the major transporter underlying transcellular absorption, (16, 39), the normal P_i homeostasis observed in NaPi-IIb KO animals and PAM patients can only be explained by the presence of additional pathways for P_i absorption (5). NaPi-IIb may account for approximately 50% of P_i transport in everted gut sacs in the presence of 1.2 mM P_i (39). However, these experiments might rather reflect the maximal contribution of a fully saturated NaPi-IIb, since generally luminal P_i content is considered to be much higher. NaPi-IIb KO mice are able to maintain P_i homeostasis when luminal P_i content is high, but develop problems to maintain P_i homeostasis as soon as dietary P_i is restricted and NaPi-IIb becomes crucial to scavenge low amounts of P_i in the gut (27).

Passive diffusion of P_i across the intestinal epithelium has been described decades ago, but has remained mostly uncharacterized. Here, we found that luminal concentrations of P_i in intestine from mice fed standard chow were in the 20 mM range and exceed plasma levels several fold. Other reports have found similar luminal concentrations of P_i up to 17 mM in humans (6), around 6.5 mM in rat tissue (32) and up to 40 mM in mice (23), all of them exceeding plasma concentration of P_i severalfold providing a sufficient gradient to drive a passive absorption process. Thus, the intestinal P_i content is also much higher than the apparent K_m of NaPi-IIb for P_i (about 10 µM) (9). Although NaPi-IIb would be already saturated, intestinal transport is still able to increase in response to high dietary P_i, as reflected by increased phosphaturia in NaPiIIb KO mice (27) and an almost linear relationship between luminal P_i content and absorbed P_i in humans (7).

Here, we were able to demonstrate using both dilution potential measurements and radiolabeled flux experiments that the tight junctions of intestinal cell culture models as well as of native tissue (rat and mouse intestine) are highly permeable to P_i. Observed P_{Pi} were similar when P_i was applied to either the apical or the basolateral side. The same was true for fluxes of radiolabeled Pi, where the same amount of P_i could be detected on the other side independent from which side the tracer was originally added. Observed transport rates increased in a linear fashion with

increasing amounts of P_i (up to 70 mM) without any saturation as it had been already described decades ago (33). Both the symmetry of transport and the linear increase with increasing concentrations of the substrate are hallmarks of simple diffusion, on which paracellular absorption relies on. In contrast, active transport depending on two distinct transport steps to pass the apical and basolateral membrane of intestinal cells is hardly symmetric and follows Michaelis Menten kinetics, saturating at particular substrate concentrations. Additionally, dilution potential and radiolabeled flux measurements provided comparable P_{Pi} values. All intestinal segments showed similar permeability of P_i in comparison to Na^+, including colon, though absolute P_{Pi} was lower in colon due to an increase in transepithelial resistance. Although many studies pointed to a higher active absorptive capacity for P_i in the small intestine (32), hyperphosphatemia also develops after enemas containing P_i concentrations exceeding blood levels, highlighting the capacity of the colon to absorb P_i (22). However, the physiological role of the colon in intestinal P_i absorption might be minor, due to increasing solidity of the content.

Of interest, paracellular transport was slightly more selective for monovalent than for divalent P_i, since both absolute (P_{Pi}) and relative (P_{Pi}/P_{Na}) permeability for P_i consistently decreased with alkaline pH, whereas there was no or only a mild effect of pH on the permeabilities for Na^+ and Cl^-. Intestinal pH varies along the intestinal lumen between 6 and 8, with more alkaline conditions towards the end of the small intestine and more acidic at the beginning of the small intestine and in the colon. At intermediate pH values both monovalent and divalent P_i are present in the lumen. Our data suggests that monovalent P_i would be slightly better absorbed via the paracellular route. In contrast, divalent P_i is the preferred substrate of NaPi-IIb (9) and would be rather absorbed transcellularly. This pattern of preferences would allow a higher absorption in the proximal small intestine, where lower pH and presumably higher concentrations of P_i would drive paracellular absorption.

The molecular mechanism responsible for paracellular P_i permeability remains unknown, since until now none of the tight junction proteins has been reported to act as a channel for P_i. A recent study showed regulation of several claudins on mRNA and protein level in NaPi-IIb deficient mice (23). However, the physiological implication of these changes should be further investigated, especially, since we did not detect major differences in the permeability of the intestine to P_i in NaPi-IIb

deficient mice suggesting that the paracellular pathway does not adapt to compensate for NaPi-IIb deficiency.

The potential therapeutic effects of inhibiting NaPi-IIb to correct hyperphosphatemia in CKD is controversially discussed (10, 28, 30, 40), especially considering that the absence of NaPi-IIb alone was not able to fully correct inappropriately high Pi blood levels in an adenine induced CKD model (40). This was only possible in conjunction with sevelamer, a Pi binder. On the other hand, sevelamer alone upregulated the expression of NaPi-IIb (40). Thus, future therapies aiming at reducing intestinal P_i absorption may target both components, the active NaPiIIb-mediated transcellular transport, as well as the paracellular pathway (10). Identification of its properties and the molecules underlying this pathway will be important.

In summary we demonstrate that the intestinal tight junctions are highly permeable to P_i and provide a major route for passive P_i absorption in the gut. Paracellular P_i permeability is substantial, amounting to about 50% of Na^+ permeability, and unlike the active transport does not change along the intestinal tract. Further, tight junctions partially discriminate between the two P_i species available under physiological conditions favoring monovalent over divalent P_i. Our findings from dilution potential measurements were validated with $^{32}P_i$ flux experiments. The relative contribution of each, active and passive, component of intestinal P_i transport to overall intestinal P_i absorption remains to be determined. Our and previous findings (39) suggest that under normal dietary conditions the contribution of paracellular absorption of Pi dominates, whereas NaPi-IIb is required once the chemical gradient across the intestinal epithelium is not sufficient to drive passive diffusion. Paracellular Pi absorption may also be considered as an option to save energy for Pi absorption as it does not directly depend on ATP or other energy equivalents.

Funding

This study was supported by a grant from the Swiss National Science Foundation (31003A_176125) to C.A.Wagner and the Hartmann Müller – Stiftung to N. Hernando.

Disclosure

C.A.Wagner has received honoraria for lectures and participating in an advisory board from Medice. All other authors declare no conflict of interests.

Figure legends

Figure 1: Intestinal P_i-content und paracellular pH-dependent Na^+, Cl^- and P_i permeabilities of intestinal cell models

Luminal content of P_i along the intestinal tract of WT mice (**A**) exceeds plasma levels (≈2 mM), providing a gradient for passive absorption of Pi (n=3-6 mice/segment). Transepithelial resistance in different intestinal cell culture models (**B**) is decreased at pH 8.4 compared to pH 6. The permeability ratio P_{Na}/P_{Cl} in intestinal cell culture models (**C**) was not affected by pH, whereas pH 8.4 reduced the ratio P_{Pi}/P_{Na} (**D**) in all cell models tested. Data is presented as mean + SD (n=6-13), and was analyzed by grouped two-way ANOVA-Bonferroni. Significances are indicated as ***p<0.001 and mark differences between pH 6 and pH 8.4.

Figure 2: P_i-permeability of rat intestinal segments

Transepithelial resistance in jejunum, ileum and colon from rat (**A**) is not affected by pH. The permeability ratio P_{Na}/P_{Cl} (**B**) was not affected by pH in jejunum and ileum, but increased in colon at pH 8.4. The permeability ratio P_{Pi}/P_{Na} (**C**) is reduced at pH 8.4 in all tissues. Absolute permeabilities for Na^+ (**D**) and Cl^- (**E**) were not affected by pH in all tissues, whereas P_{Pi} (**F**) was decreased in ileum at pH 8.4. Data is presented as mean + SD (n=12), and was analyzed by grouped two-way ANOVA-Bonferroni. Significances are indicated as *p<0.05, ***p<0.001 and mark differences between pH 6 and pH 8.4.

Figure 3: Concentration and pH-dependent accumulation and fluxes of radiolabeled Pi across rat jejunum.

$^{32}P_i$ flux experiments at pH 6 in rat jejunum applying a gradient (**A**) of 10 mM, 35 mM or 70 mM, respectively, from the apical to the basolateral side or keeping the same substrate concentration on both sides (**B**) resulted in a time-dependent and linear increase of radiolabeled Pi at the basolateral side. Average fluxes from each experiment (average from 1 to 4 hours time points) increase in an almost linear

fashion with increasing substrate concentrations (**C**). Applying an apical to basolateral or basolateral to apical gradient of P_i resulted in both conditions in a similar Pi-flux (**D**). P_i flux experiments at pH 8.4 in rat jejunum applying a gradient of 10 and 35 mM from the apical to the basolateral side also resulted in a time-dependent and linear increase of radiolabeled P_i at the basolateral side (**E**). Fluxes at pH 8.4 increase with substrate concentration as observed at pH 6 but at lower rates (**F**). Comparison of Pi translocated to the acceptor sitein presence of a gradient of 10 and 35 mM from apical to the basolateral side at pH 6 and 8.4 indicated lower amounts of Pi detected on the basolateral side at pH 8.4 (**G**). Absolute permeability for P_i (P_{Pi}) obtained from flux experiments (at the two hours' time point) (**H**) and from the dilution potential measurements (**I**) showed lower P_{Pi} at pH 8.4 and provided comparable results. Data is presented as mean ± SD (n=4-7), linear regression line and was analyzed by grouped two-way ANOVA-Bonferroni (A-G) or unpaired t-test (H-I). Significances are indicated as *p<0.05, **p<0.01, ***p<0.001 and mark differences between pH 6 and pH 8.4.

Figure 4: Dilution potential measurements are similar in intestinal segments of WT and NaPi-IIb mice.

Transepithelial resistance values in duodenum, jejunum, ileum and colon of WT and NaPi-IIb KO mice (**A**): no differences were observed between genotypes. Absolute permeabilities P_{Na} (**B**), P_{Cl} (**C**) and P_{Pi} (**D**) inversely correlated with tissue resistance, being slightly lower in duodenum and colon compared to distal small intestine, but no significant differences between genotypes were observed. Relative permeabilities P_{Na}/P_{Cl} (E) and P_{Na}/P_{Pi} (F) were comparable between KO and WT animals. Data is presented as mean ± SD (n=4-5), and was analyzed by grouped two-way ANOVA-Bonferroni.

Figure 5: Fluxes of radiolabeled P_i in mouse small and large intestine are similar in WT and NaPi-IIb KO animals

Flux of Radiolabeled Pi in duodenum (**A**), jejunum (**B**), ileum (**C**) and colon (**D**) in WT and KO mice in presence of 70 mM Pi at the luminal site of the tissue (pH 6).Data is presented as mean ± SD (n=6-8), and analyzed with unpaired t-test.

References

1. **Alizadeh Naderi AS, and Reilly RF**. Hereditary disorders of renal phosphate wasting. *Nat Rev Nephrol* 6: 657-665, 2010.
2. **Bergwitz C, and Juppner H**. Regulation of phosphate homeostasis by PTH, vitamin D, and FGF23. *Annu Rev Med* 61: 91-104, 2010.
3. **Calvo MS**. Dietary considerations to prevent loss of bone and renal function. *Nutrition* 16: 564-566, 2000.
4. **Capuano P, Radanovic T, Wagner CA, Bacic D, Kato S, Uchiyama Y, St-Arnoud R, Murer H, and Biber J**. Intestinal and renal adaptation to a low-Pi diet of type II NaPi cotransporters in vitamin D receptor- and 1alphaOHase-deficient mice. *Am J Physiol Cell Physiol* 288: C429-434, 2005.
5. **Corut A, Senyigit A, Ugur SA, Altin S, Ozcelik U, Calisir H, Yildirim Z, Gocmen A, and Tolun A**. Mutations in SLC34A2 cause pulmonary alveolar microlithiasis and are possibly associated with testicular microlithiasis. *Am J Hum Genet* 79: 650-656, 2006.
6. **Davis GR, Zerwekh JE, Parker TF, Krejs GJ, Pak CY, and Fordtran JS**. Absorption of phosphate in the jejunum of patients with chronic renal failure before and after correction of vitamin D deficiency. *Gastroenterology* 85: 908-916, 1983.
7. **Davis GR, Zerwekh JE, Parker TF, Krejs GJ, Pak CYC, and Fordtran JS**. Absorption of Phosphate in the Jejunum of Patients with Chronic-Renal-Failure before and after Correction of Vitamin-D Deficiency. *Gastroenterology* 85: 908-916, 1983.
8. **Fiske CH, and Subbarow Y**. The colorimetric determination of phosphorus. *J Biol Chem* 66: 375-400, 1925.
9. **Forster IC, Virkki L, Bossi E, Murer H, and Biber J**. Electrogenic kinetics of a mammalian intestinal type IIb Na(+)/P(i) cotransporter. *J Membr Biol* 212: 177-190, 2006.
10. **Fouque D, Vervloet M, and Ketteler M**. Targeting Gastrointestinal Transport Proteins to Control Hyperphosphatemia in Chronic Kidney Disease. *Drugs* 2018.
11. **Frizzell RA, and Schultz SG**. Ionic conductances of extracellular shunt pathway in rabbit ileum. Influence of shunt on transmural sodium transport and electrical potential differences. *J Gen Physiol* 59: 318-346, 1972.
12. **Greger R**. Cation selectivity of the isolated perfused cortical thick ascending limb of Henle's loop of rabbit kidney. *Pflugers Arch* 390: 30-37, 1981.
13. **Grundy D**. Principles and standards for reporting animal experiments in The Journal of Physiology and Experimental Physiology. *J Physiol-London* 593: 2547-2549, 2015.
14. **Gunzel D, and Yu AS**. Claudins and the modulation of tight junction permeability. *Physiol Rev* 93: 525-569, 2013.
15. **Hattenhauer O, Traebert M, Murer H, and Biber J**. Regulation of small intestinal Na-P(i) type IIb cotransporter by dietary phosphate intake. *Am J Physiol Gastro Liver* 277: G756-762, 1999.
16. **Hernando N, Myakala K, Simona F, Knopfel T, Thomas L, Murer H, Wagner CA, and Biber J**. Intestinal Depletion of NaPi-IIb/Slc34a2 in Mice: Renal and Hormonal Adaptation. *J Bone Miner Res* 30: 1925-1937, 2015.
17. **Hernando N, and Wagner CA**. Mechanisms and Regulation of Intestinal Phosphate Absorption. *Compr Physiol* 8: 1065-1090, 2018.

18. **Hilfiker H, Hattenhauer O, Traebert M, Forster I, Murer H, and Biber J**. Characterization of a murine type II sodium-phosphate cotransporter expressed in mammalian small intestine. *Proc Nat Acad Sci US A* 95: 14564-14569, 1998.
19. **Himmerkus N, Vassen V, Sievers B, Goerke B, Shan Q, Harder J, Schroder JM, and Bleich M**. Human beta-defensin-2 increases cholinergic response in colon epithelium. *Pflugers Arch* 460: 177-186, 2010.
20. **Hruska KA, Mathew S, Lund R, Qiu P, and Pratt R**. Hyperphosphatemia of chronic kidney disease. *Kidney Int* 74: 148-157, 2008.
21. **Hu MC, Shiizaki K, Kuro-o M, and Moe OW**. Fibroblast growth factor 23 and Klotho: physiology and pathophysiology of an endocrine network of mineral metabolism. *Annu Rev Physiol* 75: 503-533, 2013.
22. **Hu MS, Kayne LH, Jamgotchian N, Ward HJ, and Lee DBN**. Paracellular phosphate absorption in rat colon: A mechanism for enema-induced hyperphosphatemia. *Miner Electrol Metab* 23: 7-12, 1997.
23. **Ikuta K, Segawa H, Sasaki S, Hanazaki A, Fujii T, Kushi A, Kawabata Y, Kirino R, Sasaki S, Noguchi M, Kaneko I, Tatsumi S, Ueda O, Wada NA, Tateishi H, Kakefuda M, Kawase Y, Ohtomo S, Ichida Y, Maeda A, Jishage KI, Horiba N, and Miyamoto KI**. Effect of Npt2b deletion on intestinal and renal inorganic phosphate (Pi) handling. *Clin Exp Nephrol* 22: 517-528, 2018.
24. **Karp HJ, Vaihia KP, Karkkainen MUM, Niemisto MJ, and Lamberg-Allardt CJE**. Acute effects of different phosphorus sources on calcium and bone metabolism in young women: A whole-foods approach. *Calcified Tissue Int* 80: 251-258, 2007.
25. **Katai K, Miyamoto K, Kishida S, Segawa H, Nii T, Tanaka H, Tani Y, Arai H, Tatsumi S, Morita K, Taketani Y, and Takeda E**. Regulation of intestinal Na^+-dependent phosphate co-transporters by a low-phosphate diet and 1,25-dihydroxyvitamin D-3. *Biochem J* 343: 705-712, 1999.
26. **Kimizuka H, and Koketsu K**. Ion Transport through Cell Membrane. *J Theor Biol* 6: 290-&, 1964.
27. **Knopfel T, Pastor-Arroyo EM, Schnitzbauer U, Kratschmar DV, Odermatt A, Pellegrini G, Hernando N, and Wagner CA**. The intestinal phosphate transporter NaPi-IIb (Slc34a2) is required to protect bone during dietary phosphate restriction. *Sci Rep* 7: 11018, 2017.
28. **Larsson TE, Kameoka C, Nakajo I, Taniuchi Y, Yoshida S, Akizawa T, and Smulders RA**. NPT-IIb Inhibition Does Not Improve Hyperphosphatemia in CKD. *Kidney Int Rep* 3: 73-80, 2018.
29. **Layunta E, Pastor Arroyo EM, Kägi L, Thomas L, Levi M, Hernando N, and Wagner CA**. Intestinal response to acute intragastric and intravenous administration of phosphate in rats. *Cell Physiol Biochem* in press: 2019.
30. **Lenglet A, Liabeuf S, Guffroy P, Fournier A, Brazier M, and Massy ZA**. Use of nicotinamide to treat hyperphosphatemia in dialysis patients. *Drugs in R&D* 13: 165-173, 2013.
31. **Lien YHH**. Phosphorus: Another Devil in Our Diet? *Am J Med* 126: 280-281, 2013.
32. **Marks J, Lee GJ, Nadaraja SP, Debnam ES, and Unwin RJ**. Experimental and regional variations in Na+-dependent and Na+-independent phosphate transport along the rat small intestine and colon. *Physiol Rep* 3: 2015.
33. **McHardy GJR, and Parsons DS**. THE ABSORPTION OF INORGANIC PHOSPHATE FROM THE SMALL INTESTINE OF THE RAT. *Q J Exp Physiol Cogn Med Sci* 41: 398-409, 1956.
34. **Nordin BEC**. *Calcium, Phosphate, and Magnesium Metabolism: Clinical Physiology and Diagnostic Procedures*. Churchill Livingstone, 1976.

35. **Paloian NJ, and Giachelli CM**. A current understanding of vascular calcification in CKD. *Am J Physiol Renal* 307: F891-900, 2014.
36. **Radanovic T, Wagner CA, Murer H, and Biber J**. Regulation of intestinal phosphate transport. I. Segmental expression and adaptation to low-P(i) diet of the type IIb Na(+)-P(i) cotransporter in mouse small intestine. *Am J Physiol Gastro Liver* 288: G496-500, 2005.
37. **Razzaque MS**. Phosphate toxicity: new insights into an old problem. *Clin Sci* 120: 91-97, 2011.
38. **Rosenthal R, Gunzel D, Krug SM, Schulzke JD, Fromm M, and Yu AS**. Claudin-2-mediated cation and water transport share a common pore. *Acta Physiol (Oxf)* 2016.
39. **Sabbagh Y, O'Brien SP, Song W, Boulanger JH, Stockmann A, Arbeeny C, and Schiavi SC**. Intestinal npt2b plays a major role in phosphate absorption and homeostasis. *J Am Soc Nephrol* 20: 2348-2358, 2009.
40. **Schiavi SC, Tang W, Bracken C, O'Brien SP, Song WP, Boulanger J, Ryan S, Phillips L, Liu SG, Arbeeny C, Ledbetter S, and Sabbagh Y**. Npt2b Deletion Attenuates Hyperphosphatemia Associated with CKD. *J Am Soc Nephrol* 23: 1691-1700, 2012.
41. **Shibasaki Y, Etoh N, Hayasaka M, Takahashi MO, Kakitani M, Yamashita T, Tomizuka K, and Hanaoka K**. Targeted deletion of the tybe IIb Na(+)-dependent Pi-co-transporter, NaPi-IIb, results in early embryonic lethality. *Biochem Biophys Res Commun* 381: 482-486, 2009.
42. **Wagner CA, Rubio-Aliaga I, and Hernando N**. Renal phosphate handling and inherited disorders of phosphate reabsorption: an update. *Pediatr Nephrol* 2017.
43. **Walling MW, Brautbar N, and Coburn JW**. Jejunal Phosphate (Pi) Active-Transport - Effects of Phosphorus Depletion and Vitamin-D. *Fed Proc* 36: 1097-1097, 1977.
44. **Walton J, and Gray TK**. Absorption of Inorganic-Phosphate in the Human Small-Intestine. *Clin Sci* 56: 407-412, 1979.

Figure 1

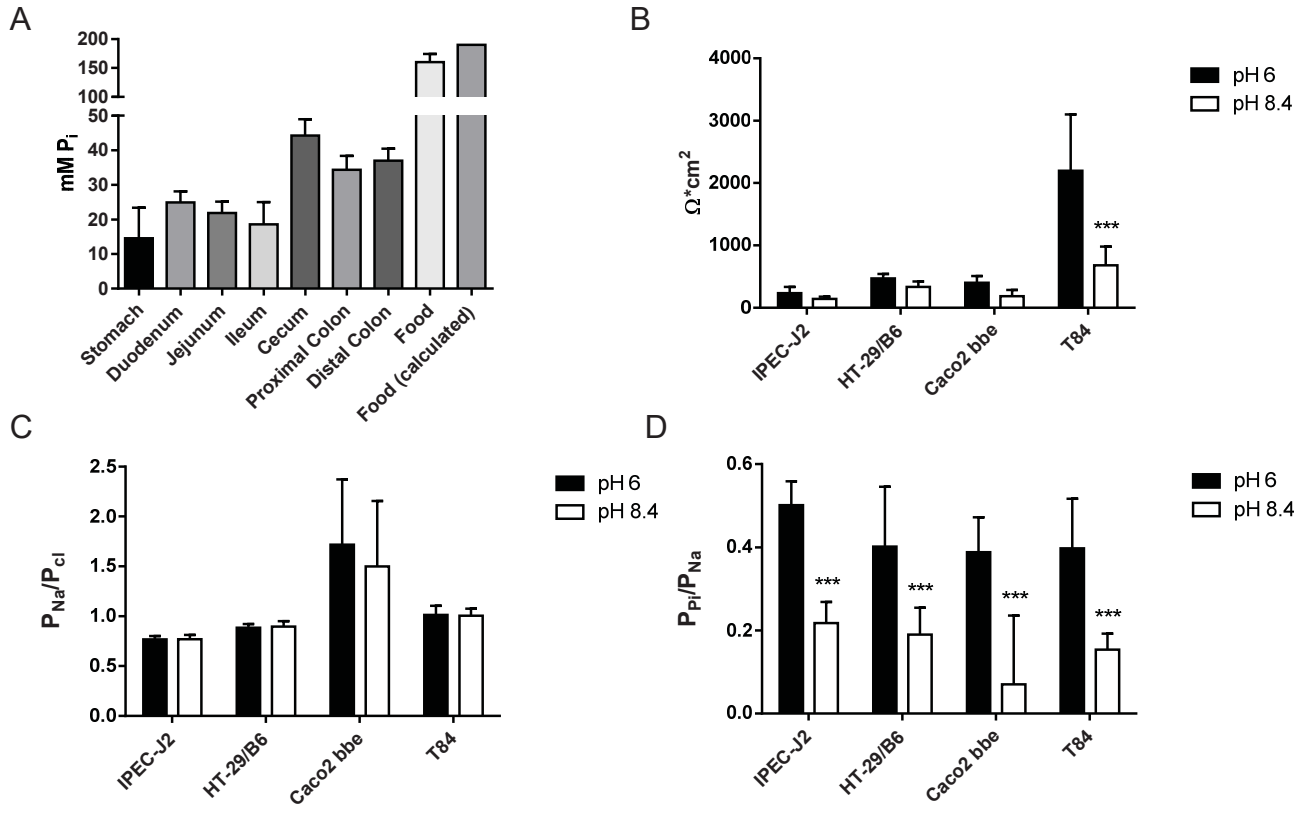
A
mM P_i
200
150
100
50
40
30
20
10
0
Stomach
Duodenum
Jejunum
Ileum
Cecum
Proximal Colon
Distal Colon
Food
Food (calculated)
B
$\Omega*cm^2$
4000
3000
2000
1000
0
***
IPEC-J2
HT-29/B6
Caco2 bbe
T84
pH 6
pH 8.4
C
P_{Na}/P_{cl}
2.5
2.0
1.5
1.0
0.5
0.0
IPEC-J2
HT-29/B6
Caco2 bbe
T84
pH 6
pH 8.4
D
P_{Pi}/P_{Na}
0.6
0.4
0.2
0.0
***
IPEC-J2
HT-29/B6
Caco2 bbe
T84
pH 6
pH 8.4

Figure 2

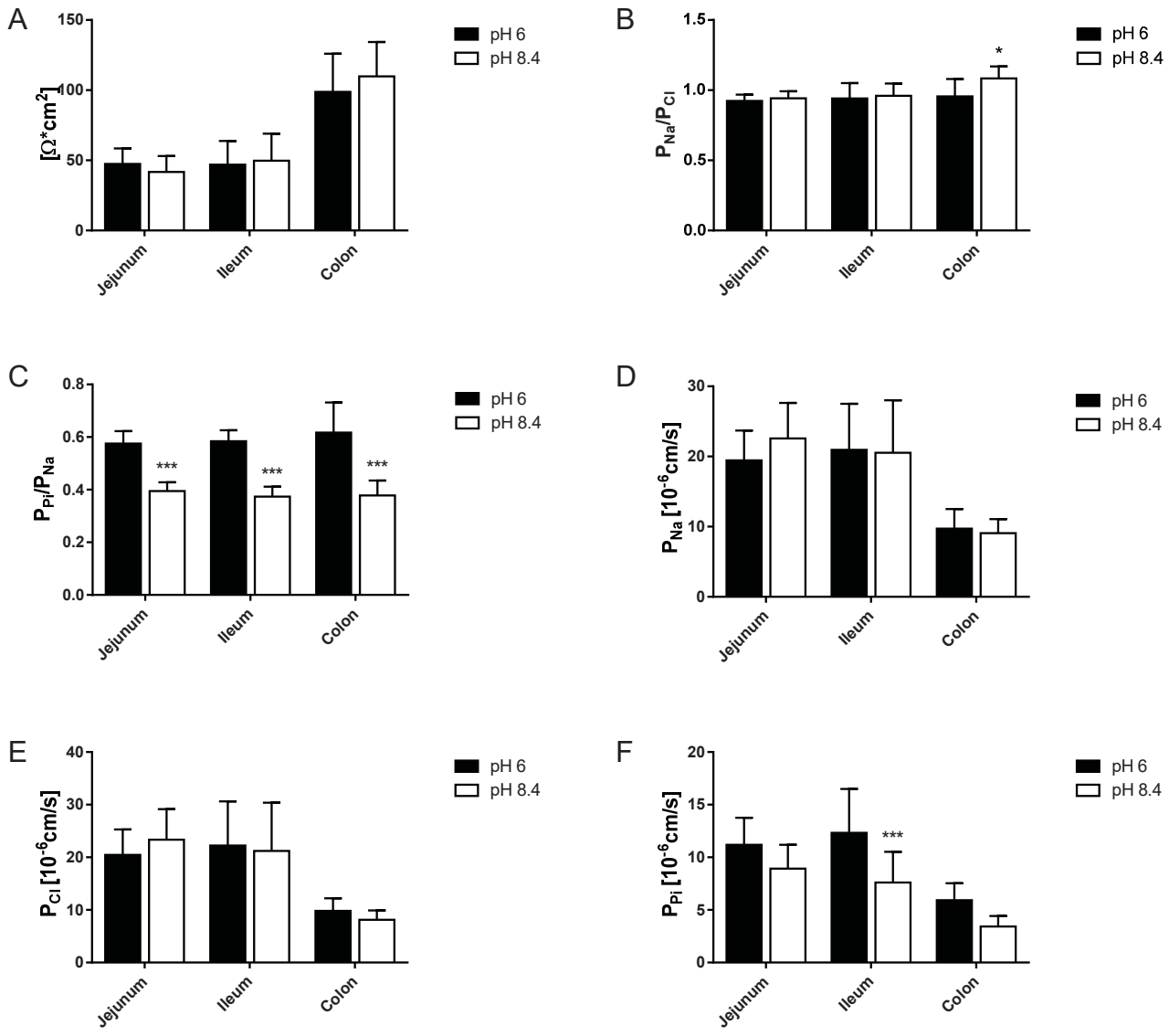
A
150
100
50
0
[Ω*cm²]
pH 6
pH 8.4
Jejunum
Ileum
Colon
B
1.5
1.0
0.5
0.0
P_Na/P_Cl
*
C
0.8
0.6
0.4
0.2
0.0
P_Pi/P_Na
***
D
30
20
10
0
P_Na [10⁻⁶cm/s]
E
40
30
20
10
0
P_Cl [10⁻⁶cm/s]
F
20
15
10
5
0
P_Pi [10⁻⁶cm/s]

Figure 3

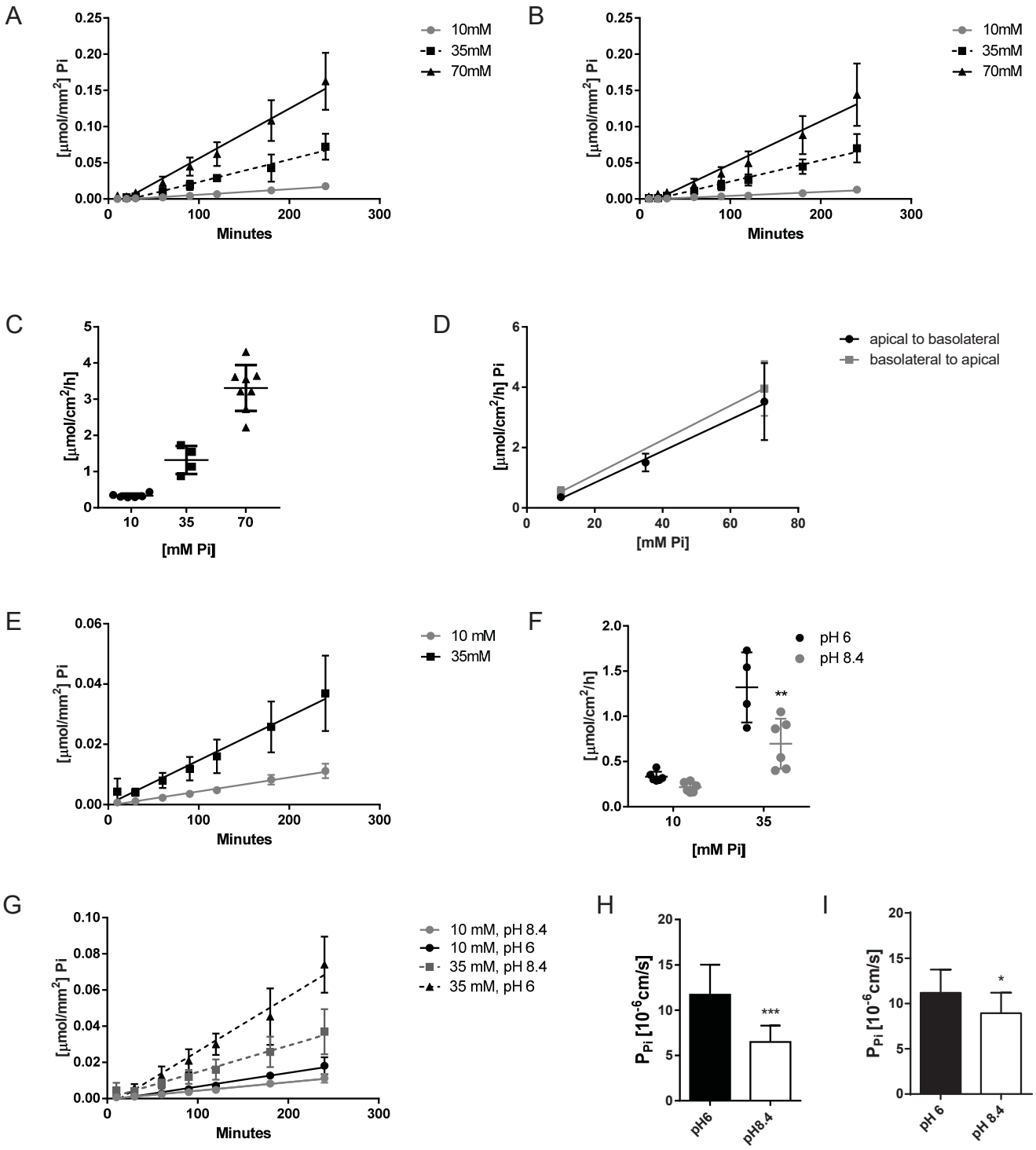
A
B
C
D
E
F
G
H
I
10mM
35mM
70mM
Minutes
[µmol/mm2] Pi
[µmol/cm2/h]
[mM Pi]
apical to basolateral
basolateral to apical
10 mM
35mM
pH 6
pH 8.4
**
10 mM, pH 8.4
10 mM, pH 6
35 mM, pH 8.4
35 mM, pH 6
PPi [10-6cm/s]
***
*
pH6
pH8.4

Figure 4

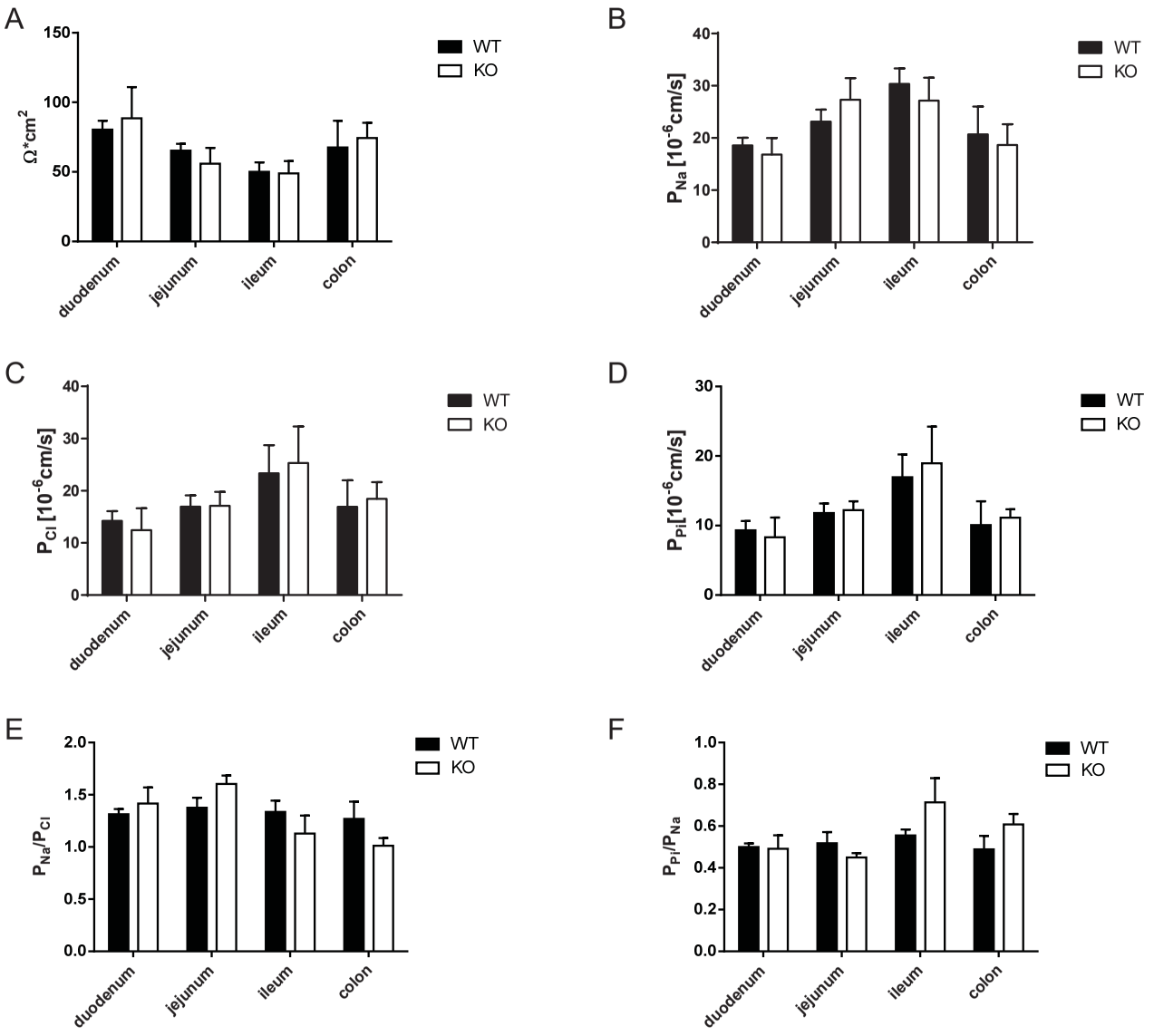
A
150
100
50
0
Ω*cm²
WT
KO
duodenum
jejunum
ileum
colon
B
40
30
20
10
0
P_Na [10⁻⁶cm/s]
WT
KO
duodenum
jejunum
ileum
colon
C
40
30
20
10
0
P_Cl [10⁻⁶cm/s]
WT
KO
duodenum
jejunum
ileum
colon
D
30
20
10
0
P_Pi[10⁻⁶cm/s]
WT
KO
duodenum
jejunum
ileum
colon
E
2.0
1.5
1.0
0.5
0.0
P_Na/P_Cl
WT
KO
duodenum
jejunum
ileum
colon
F
1.0
0.8
0.6
0.4
0.2
0.0
P_Pi/P_Na
WT
KO
duodenum
jejunum
ileum
colon

Figure 5